Innovative Shade Mitigation Technique for Maximizing Solar Energy Efficiency in Roof-Mounted PV Systems

Nawal Cheggaga[1], Khadidja Dahli[2], Mohamed Rafik Hammouda[2], Abdellah Benallal[3], Adrian Ilinca[4*]

[1] Department of Electronics, University of Blida 1, Blida 09000, Algeria
[2] Department of Automatic and Electrotechnical, University of Blida 1, Blida 09000, Algeria
[3] Department of Engineering, University of Quebec at Rimouski, Quebec G5L 2Z9, Canada
[4] Department of Mechanical Engineering, Ecole de Technologies Supérieure, Quebec H3C 1K3, Canada

Corresponding Author Email: adrian.ilinca@etsmtl.ca

ABSTRACT

Shading in photovoltaic (PV) systems can reduce power output, cause hot spots, efficiency losses, maintenance needs, and impact economic returns. Traditional shading solutions for PV systems are complex and expensive, requiring advanced sensors, imaging technologies, and complicated algorithms. This study presents a cost-effective, simple method that does not rely on sensors, cameras, or complex systems. It involves a site assessment to identify shading sources and precise shadow length calculations using astronomical equations. By combining site analysis with tracking mechanisms, the system proactively avoids shading with minimal energy loss, only 2.7% of the generated energy. Unlike other techniques that react to shading, this approach focuses on predicting and preventing shading, ensuring optimal performance. A prototype of the system demonstrated efficient sun tracking and shading avoidance. This innovative approach improves PV efficiency, reduces costs, and promotes adoption due to its simplicity and scalability.

1. INTRODUCTION

Buildings account for almost 40% of energy consumption globally [1]. Therefore, enabling buildings to manage their energy demand and production is one of the ultimate goals of the world [2]. Roof-mounted solar PV systems are the most efficient and clean systems enabling buildings to produce power. Since sunlight is the power source for a solar PV system, shading is an important factor in choosing the right spot to place modules, as it can significantly reduce the entire system's efficiency. Even a single shaded cell in a long string of cells can easily cut over half the output power [3]. Some of the typical shade sources that can reduce a PV system's output power are chimneys, trees, and other roofs [4], see Figure 1. Clouds are another source of shading but do not affect the efficiency of PV arrays as nearby objects [5]. Therefore, minimizing shading through careful site selection and panel positioning is crucial for optimizing solar panel efficiency and maximizing energy production. This imperative step ensures the efficient harnessing of solar energy and holds the key to revolutionizing building energy consumption and shaping the future of sustainable architecture.

Shading detrimentally impacts solar panel efficiency by obstructing sunlight, the primary energy source for solar photovoltaic (PV) systems. When shaded, even partially, solar panels experience reduced sunlight exposure, leading to decreased energy production [6, 7].

This reduction occurs due to the interconnected nature of solar cells within the panel; if only 20% of the surface of the solar panel is shaded, 50% of the output of the entire array can be reduced [8]. Consequently, shading from objects like trees, nearby buildings, or even clouds can significantly hinder the performance of solar panels. Research has indicated that for each 10% of shade on the surface, there is a 2.3% drop in electrical efficiency [9]. Moreover, shading can potentially reduce the efficiency of a system up to 99.98%, resulting in the total failure of the system [10].

The literature provides various techniques to reduce the detrimental effects of shading on solar panels. One commonly employed method is the use of bypass diodes, which serve to mitigate the impact of shading and safeguard the integrity of the solar panels [11-16]. Additionally, implementing a maximum power point tracking system can optimize the energy output of the panels despite shading [17-22]. Grouping shaded modules in separate strings, known as parallel series, is another strategy to maximize the overall output power of the photovoltaic array [23, 24]. Furthermore, the integration of DC optimizers allows for the adjustment of output voltage and current to maintain maximum power without compromising the performance of other modules in the case of partial shade [25-27]. Careful selection of materials to minimize shading [28], as well as altering the interconnection of PV arrays, are additional approaches to mitigate shading effects [29-31]. Novel methods such as dynamic reconfiguration of panel connections [32-37], modified optimization algorithms for panel layouts [38], and techniques involving renumbering and rewiring modules within the array [39], contribute to minimizing power loss from shading. Techniques like using

multiple converters [40], employing half-cell solar panels [41] [42], and maximizing power ex-traction capability through microinverters [43] or energy recovery circuits [44] are also effective in mitigating shading effects and enhancing solar panel performance.

Modern shading mitigation in PV systems involves using sensors to detect shading and adjust panel angles dynamically [45]. Some methods include using drones with advanced imaging tools to capture aerial views of large PV installations, analyze shading patterns, and optimize panel positioning [46-49]. Aerial imaging tools enhance this analysis by providing high-resolution visual data for precise mapping and proactive shading management [50-53].

(a) Chimney [46]

(b) Tree [47]

(c) Utility pole wire [48]

(d) Building [49]

**Figure 1.** Shading sources for integrated photovoltaic systems

The limitations of current shading mitigation techniques for solar panels reveal significant gaps. While bypass diode methods prevent energy loss from shaded cells, they still suffer from reduced voltage and overall energy efficiency [54, 55]. Grouping shaded modules and using multiple converters require complex modeling and simulation, which can be impractical and costly due to specialized expertise and expensive components. Sensor-based methods can only detect performance drops without pinpointing the exact shading cause or location, and drones and aerial imaging tools face limitations from weather conditions, image quality, and complexity. Shadow mapping software provides valuable data but may not reflect real-time changes, and the energy consumption of advanced techniques may outweigh their benefits.

Our novel method addresses these issues by proactively preventing shading without relying on sensors, cameras, or complex systems. Instead, it uses astronomical equations to calculate shadow lengths from potential shading sources like chimneys and trees, integrating this information into solar tracking tools. This approach enables efficient sun tracking while avoiding shaded areas. Our system achieves maximum energy production with only 2.7% of generated energy consumed, which is lower than other systems reported by Osman et al. [56] (3.4% and 3.9%), Kuttybay et al. [57] (4.2%), and Ahmad et al. [58] (5.89%), and aligns with the optimal solar tracking energy consumption range of 2-3% [59]. By simplifying the implementation process and eliminating the need for expensive technologies, this approach makes high-efficiency solar tracking more accessible for various applications. Its proactive shading prevention feature improves energy generation and system durability, potentially setting a new efficiency standard for solar tracking.

2. METHODS AND MATERIALS

2.1 Proposed solar tracking system

The solar tracker's precision is underscored by its ability to calculate key sun angles, ensuring accurate tracking of the sun's trajectory. Figure 2 visually represents the azimuth and altitude angles, showcasing how the system captures the Sun's angular displacement from the observer point (azimuth angle) and its angular height in the sky (altitude angle). These angles, calculated using precise astronomical equations, form the foundation for the solar tracker's dynamic response to the sun's movement throughout the day.
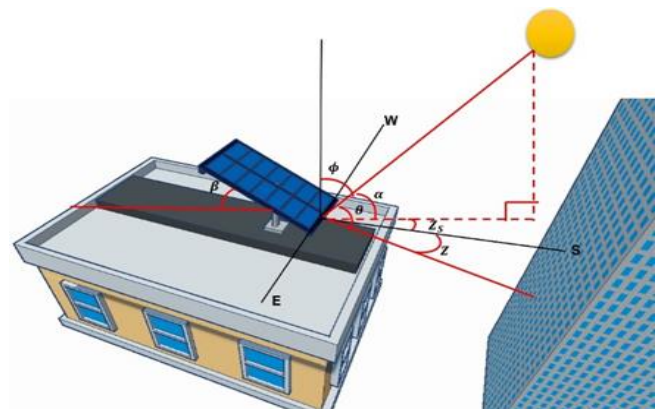
Figure 2. Sun position angles

The following equations from the Astronomical data can be used to estimate the sun's position [60].

The azimuth and altitude angles are given as:

$$Z_S = \cos^{-1}((\sin\delta \cdot \cos\phi - \cos\delta \cdot \sin\phi \cdot \cos\sigma)/\cos\alpha) \qquad (1)$$

$$\alpha = \sin^{-1}(\sin\delta \cdot \sin\varphi + \cos\delta \cdot \cos\varphi \cdot \cos\sigma) \qquad (2)$$

The angle between the Earth-Sun vector and the equatorial plane, defined as the "angle of declination," is calculated by:

$$\delta = 23.45^o \cdot \sin B \qquad (3)$$

where, B can be calculated by the number of days elapsed in a given year up to a particular date d as follows:

$$B = 360/365 \cdot (d - 81) \qquad (4)$$

The angular displacement of the Sun from the local point, known as the "hour angle," is given by:

$$\sigma = 15^o \cdot (LST-12) \qquad (5)$$

The time correction factor in minutes TC defined as the true solar time, is given by the daily apparent motion of the true or observed Sun as follows:

$$TC = 4(L\text{-}LSTM) + EoT \qquad (6)$$

The difference between apparent and mean solar times EoT is given by:

$$EoT = 9.87\sin(2B) - 7.53\cos(B) - 1.5\sin(B) \qquad (7)$$

In conjunction with precise sun angles, the solar tracker employs a mathematical model to calculate and optimize shadow length caused by front buildings. Figure 3 visually illustrates the changing shadow length, providing insights into how the solar tracker adapts to the shifting position of the sun.
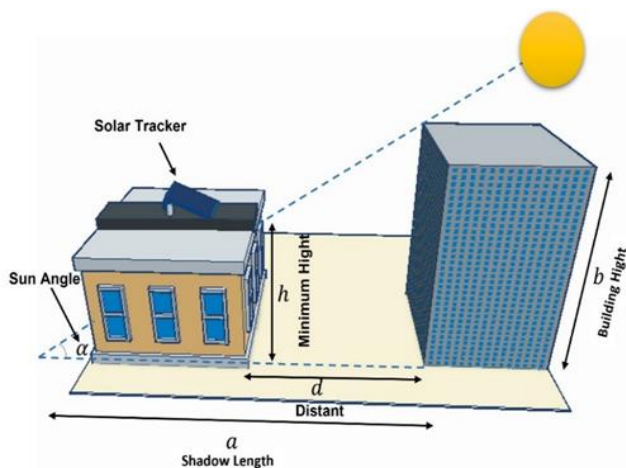

Figure 3. Shadow length of a building

When an obstacle object, such as a roof, casts a one-dimensional shadow, the length of the shadow can be calculated using a simple geometric relationship. The equation used for this calculation is:

$$a = b/\tan\alpha \qquad (8)$$

When dealing with objects that cast two-dimensional shadows, such as chimneys and trees, the calculation of the shadow length becomes more complex. In such cases, the shadow length can be determined using the following set of equations:

$$x = b(\sin(Z_S - 180)\tan(\alpha)) \qquad (9)$$

$$y = b(\cos(Z_S - 180)\tan(\alpha)) \qquad (10)$$

$$a = \sqrt{x^2 + y^2} \qquad (11)$$

2.2 Tracking system strategy

Our proposed solar tracker employs a robust strategy to optimize solar energy absorption while minimizing shadow impact, see Figure 4. Initiated by geographic coordinates, object dimensions, and the current date and time, the system utilizes advanced astronomical algorithms to calculate precise sun position angles, sunrise, sunset times, and shadow lengths. Operating within the timeframe from sunrise to sunset, the tracker periodically assesses shadow length changes. If a positive difference is detected, indicating movement away from shadows, the tracker adjusts the actuators in a counterclockwise direction.
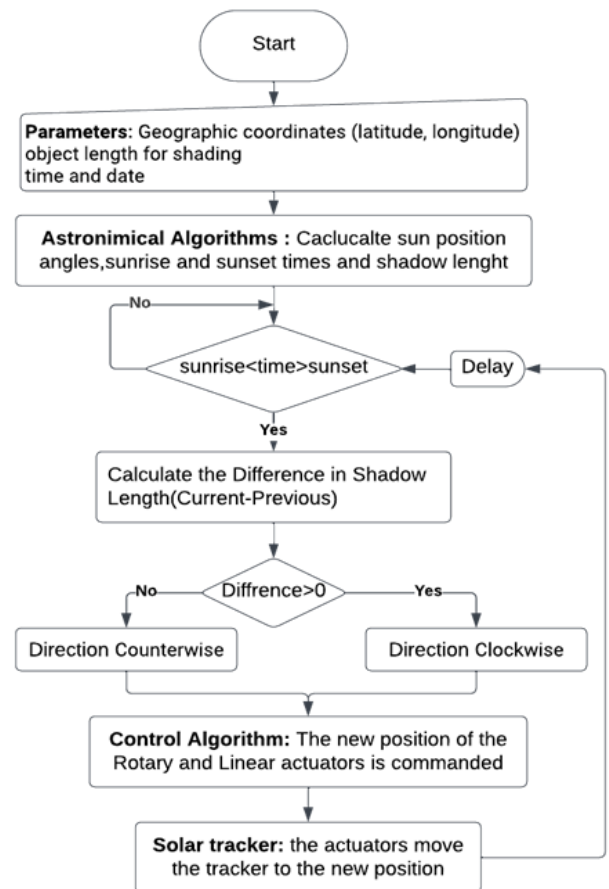

Figure 4. Flow chart of the proposed solar tracking system

Conversely, for a negative difference, signifying encroachment of shadows, the system repositions the actuators clockwise. The control algorithm then commands the rotary and linear actuators to align with the calculated sun angles, ensuring optimal exposure to sunlight while avoiding shade. This dynamic approach enhances solar energy absorption

efficiency, making the system adaptable and responsive to varying environmental conditions.

2.3 Prototype

The control unit of the proposed solar tracking system is presented in Figure 5. An Arduino microcontroller board is used to perform the tracking and avoid shading simultaneously (Number 1 in Figure 5). Two LN298 motor drives are used to drive the actuators (Number 2 in Figure 5). Two stepper motors are employed for the elevation-tracking rotary actuator and the shade-avoiding linear actuator (Number 3 in Figure 5).

The mechanical system comprises a linear actuator for moving the solar panel to prevent shading and a rotary actuator for horizontal solar tracking. The linear actuator is illustrated in Figure 6. To secure the solar panel support and prevent unintended movements, four bearings are employed (Figure 6 (a)), while two bearings above the rail facilitate smooth movement (Figure 6 (b)). A belt, connected to a stepper motor and two pulleys with a 2-meter length (1 meter outward and 1 meter return), is linked to a metal L. This L, in turn, is connected to the solar panel support (Figure 6 (c)). As the motor turns, the support undergoes translation along the rail.
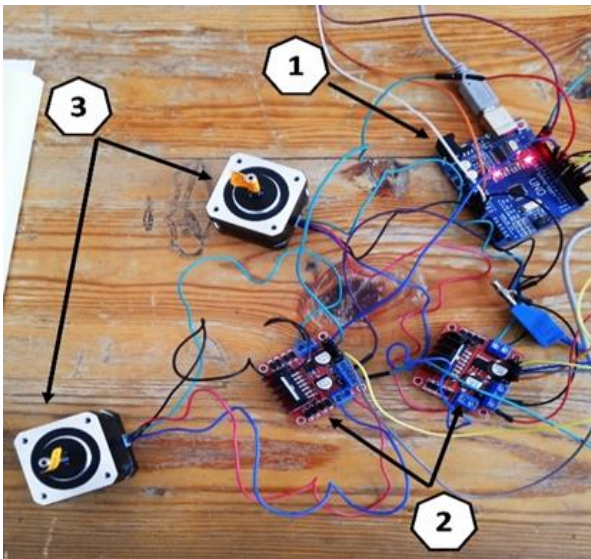
Figure 5. The proposed solar tracking control unit and prototype
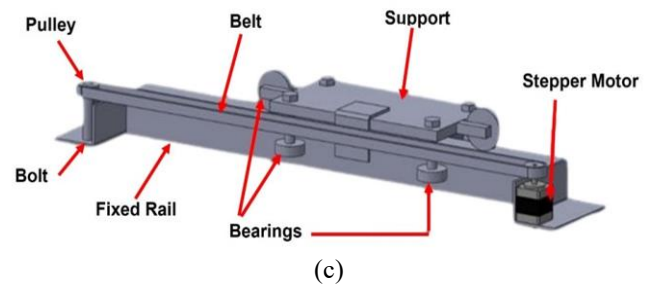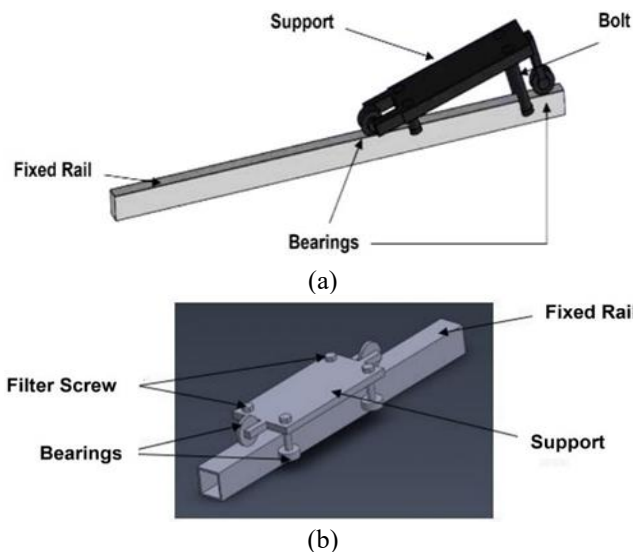
(a)

(b)

(c)

Figure 6. Linear actuator system

The rotary actuator, depicted in Figure 7, involves fixing the solar panel to a stem connected to a stepper motor. As the motor rotates, the solar panel undergoes elevation tracking.
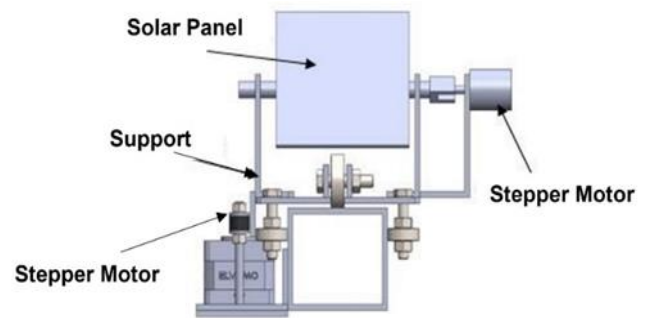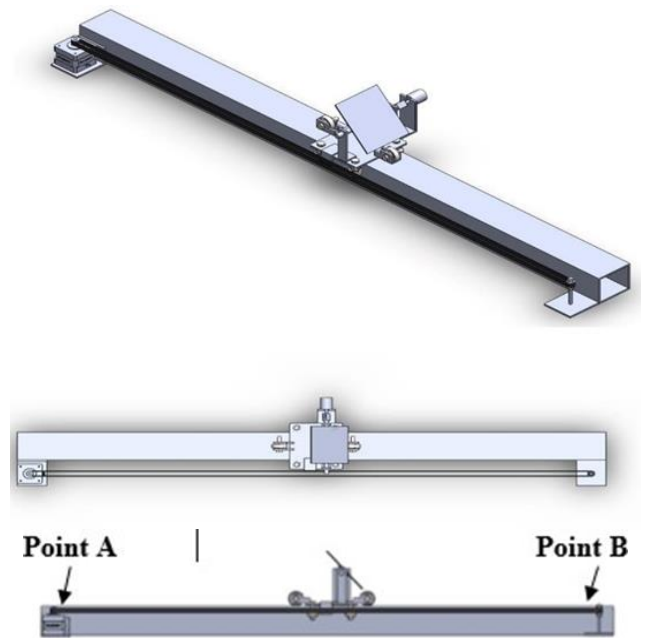
Figure 7. Rotary actuator system

**Figure 8.** The final proposed solar tracking system

The final designed solar tracker mechanism is depicted in Figure 8. Positioned initially at point B during sunrise, the tracker aligns with the sun from morning to noon. During this period, shading on the tracker diminishes gradually, reaching zero at noon. The tracker adjusts its orientation to follow the sun's path throughout this timeframe. In the afternoon, as the sun surpasses the azimuth, shading begins to cast on the tracker. To counteract this, the tracker initiates translations to prevent shading, continuing until it reaches point A at sunset. At sunset, the tracker completes its cycle and undergoes an initialization to return to position B, ready to repeat the process

the following day. Throughout this cycle, the tracker dynamically follows the sun's elevation angle, ensuring it avoids shading.

3. RESULTS AND DISCUSSIONS

The experiment was conducted at Blida 1 University, Oulad Yaich, Blida, Algeria, at 36.4225° latitude and 3.2117° longitude. The study carried out in June 2023, aimed to assess the performance of tracking systems during the peak of the summer season in Blida. The calculated sun angles at the study site are presented in Figure 9.

The figure illustrates the dynamic behavior of the Sun on June 11th, 2023, in Blida. The Sun's elevation angle follows a discernible pattern, peaking around 12:45 with an elevation of 73.62 degrees. Simultaneously, the azimuth angle exhibits systematic changes, reaching its maximum value at approximately 14:45. These variations are crucial for understanding the Sun's position in the sky throughout the day.
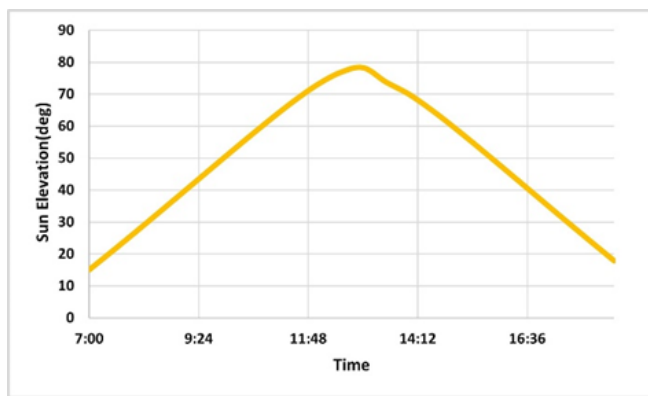
(a) Sun elevation angle
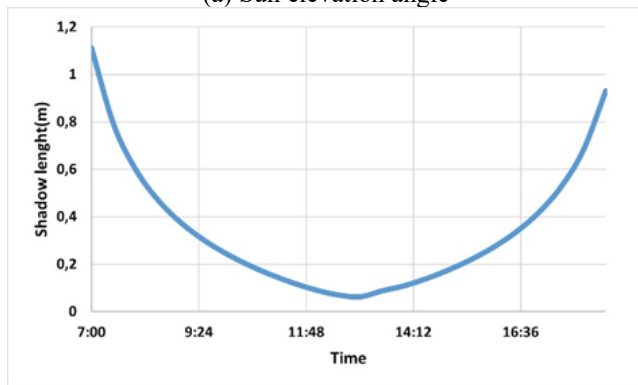
(b) Object shadow length

Figure 9. The calculated data on June the 11th 2023

The site analysis was crucial to validate the efficacy of the designed solar tracker in effectively mitigating shading from surrounding objects. The solar tracker was strategically installed atop a university roof, where an obstructing object with a height of 0.3 meters was situated in front, causing potential shading. To assess and address this challenge, the height of the building was incorporated into calculations to determine the shadow length of the object throughout the experimental day, conducted on June 11th (refer to Figure 9). Leveraging this shadow length data, the solar tracker could dynamically adjust its position, avoiding shading and optimizing solar panel orientation for enhanced energy absorption.

Figure 10 represents the real-time performance of our designed solar tracker in managing shading challenges. In the left photo, taken at 1:30 p.m., the solar tracker is shaded with a measured shadow length of 19 cm. Contrastingly, the right photo, captured at 1:45 p.m. on the same day, demonstrates the solar tracker avoiding the previously measured shadow. This dynamic adaptation showcases the tracker's capability to adjust autonomously, ensuring optimal solar panel orientation by following the sun's path. The photos' real-time nature underscores our solar tracker's practical effectiveness in mitigating shading and maximizing solar energy absorption.

Figure 11 represents the real-time adaptive rotation of the solar tracker to track the sun's changing angles. The left photo, captured at 1:45 p.m., illustrates the solar tracker's alignment with a solar altitude of 72°. In contrast, the right photo, taken at 3:00 p.m., showcases the solar tracker's adjustment to a solar altitude of 59°. The figure vividly demonstrates the solar tracker's dynamic rotation, effectively maximizing sun exposure while avoiding shading. This real-time response underscores the tracker's capability to optimize solar panel orientation for increased energy absorption and productivity.

**Figure 10.** Real-time performance of the designed solar tracker

**Figure 11.** Real-time photo of the rotation of the solar panel

The behavior of the solar tracker on the day of the experiment (June 11th, 2023) is illustrated in Figure 12. Figure 12 (a) depicts the linear actuator movement of the solar tracker, where it advances 0.38 m with each step. It is evident from the figure that the tracker remained stationary until approximately 13:00 pm. This stationary phase occurred because the object casting the shadow was positioned to the west, and its shadow did not reach the tracker until noon. Subsequently, the tracker moved forward as the shadow length increased until around 7:00 pm, corresponding to sunset. This observation underscores the importance of considering objects' position

and height when positioning the tracker to avoid shading.

Figure 12 (b) depicts the tracker's rotation actuator, representing the tilt angle. The tracker adjusts its tilt angle by 1.8° with each step based on the difference in elevation angles. It is evident from the figure that from 7:30 am to around 12:00 pm, the tracker's tilt angle remains relatively stable. This stability is attributed to the minimal sun elevation change during this period. However, around noon, the tilt angle reaches its maximum value, corresponding to the peak elevation of the sun at that time. Additionally, between 3:00 pm and 6:00 pm, the change in tilt angle is negligible. This observation suggests that discrete sun tracking, rather than real-time tracking, is more efficient. Specifically, tracking should occur three times a day: an hour before noon, at noon, and an hour after noon. This approach minimizes energy consumption while maximizing solar energy capture, as it accounts for the clear changes in elevation angles during these times.
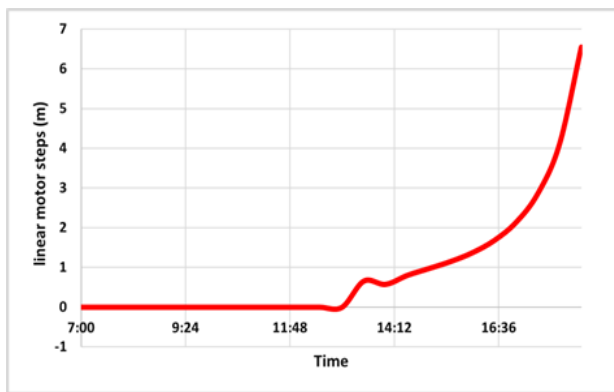
(a) The linear actuator motor position
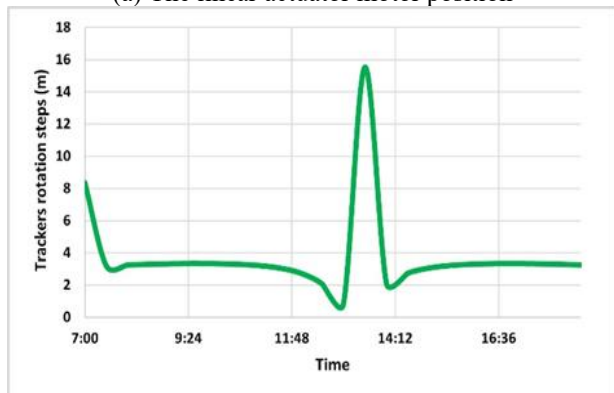
(b) The rotation motor position
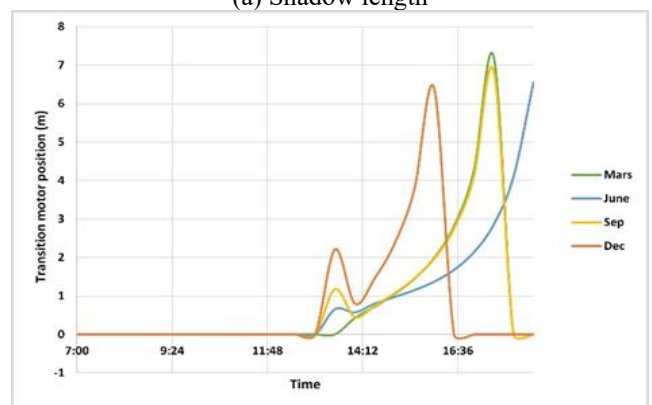
Figure 12. The solar tracker position

The behavior of the designed solar tracker was analyzed throughout each season of the year 2023 in response to changes in the sun's position and shadow length, as depicted in Figure 13. The results show that the tracker's linear actuator movement varies significantly for each season (Figure 13 (b)). This variation can be attributed to the changes in shadow length throughout the day (Figure 13 (a)), highlighting the importance of calculating shadow length continuously for successful shadow mitigation.

On the other hand, the solar tracker's rotation actuator exhibits minimal variation throughout the day (Figure 13 (d)). The only noticeable changes occur around 12:00 pm and 2:00 pm, coinciding with the sun's maximum elevation, which varies between seasons. This finding corroborates our earlier observation from the day of the experiment, where discrete sun

tracking three times a day, one hour before noon, at noon, and one hour after noon, as deemed sufficient. This underscores the non-necessity for real-time tracking, as commonly employed in sensor-based solar trackers. Implementing discrete tracking not only minimizes energy consumption but also enhances the efficiency of the PV system.
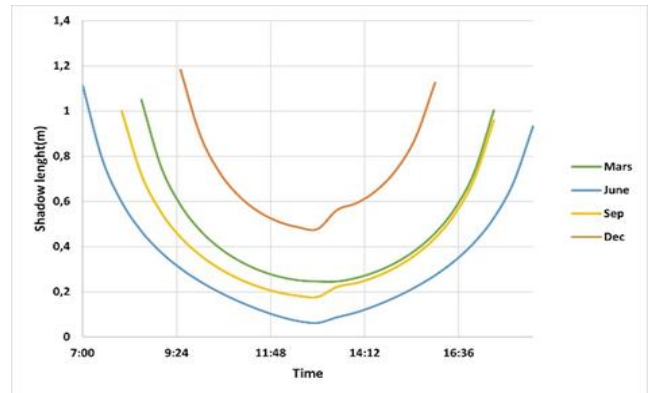
(a) Shadow length

(b) Linear motor position
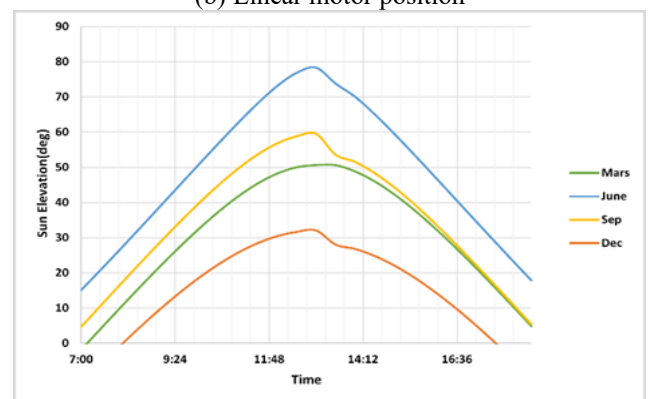
(c) Sun position

(d) Rotation motor position

Figure 13. The designed solar tracker response

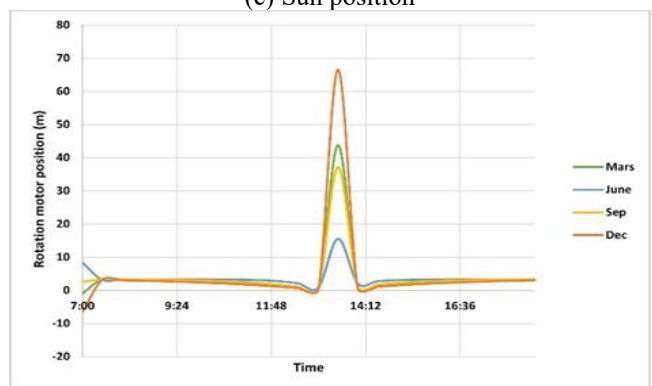During our testing, we assessed the energy production and consumption of the solar tracker on four representative seasonal days: March 11th, June 11th, September 10th, and December 17th, as shown in Figure 14. On March 11th, the solar tracker generated 14.78 watt-hours (Wh) and consumed 1.2Wh, resulting in a consumption rate of 8.14%. The low energy production was due to unclear weather conditions with a global irradiance of 5.04 kWhr/m^2 [61].
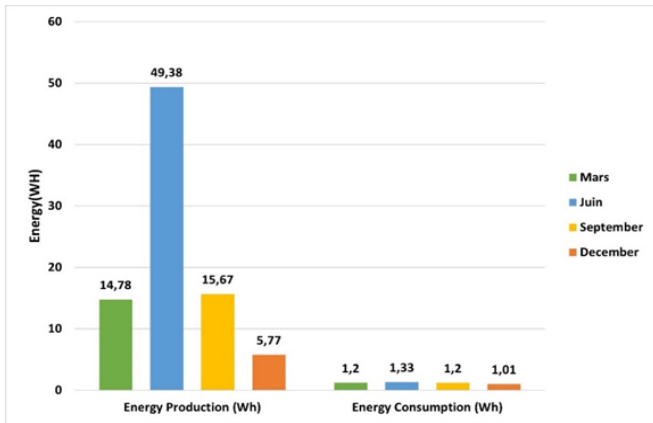
(a) Produced and consumed energy
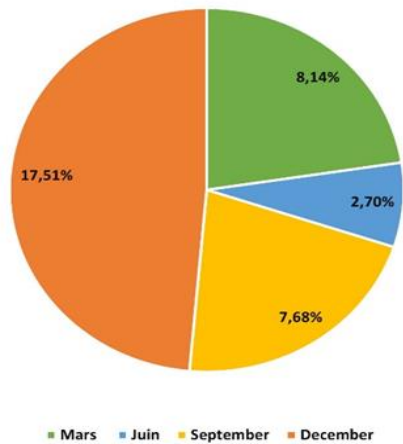
(b) Energy consumption rate in relation to produced energy

Figure 14. The designed solar tracker response

In contrast, on June 11th, energy production peaked at 49.38 WH due to clear weather and high sun intensity of 9.84kWhr/m^2 [61]. Despite a slightly longer shadow compared to March 11th, energy consumption remained low at 1.33Wh, resulting in a consumption rate of 2.7%, attributed to the high energy production.

September 10th showed similar sun position and shadow length to March 11th, resulting in a consumption rate of 7.68% with solar irradiance at 5.77kWhr/m^2 [61]. The lowest energy consumption was in December at 1.01Wh, attributed to minimal shadow length and reduced movement of the solar tracker actuator. However, energy production was significantly lower at 5.77Wh due to clouds, rain, and very low sun intensity of 2.46kWhr/m^2 [61], resulting in a consumption rate of 17.51% due to limited energy production. These results highlight the effectiveness of the solar tracker design, especially in summer. Despite the longest shadow in summer, the tracker achieved maximum power production while consuming only 2.7% of the generated energy, thanks to effective shadow avoidance and precise sun position tracking.

4. CONCLUSION

In this study, we designed a new shade-avoidant solar tracker that uses no sensors; instead, it relies on astronomical equations to follow the sun and avoid shading. The developed sensorless solar tracker demonstrates several key advantages that contribute to its effectiveness in optimizing solar energy harvesting:

(1). The tracker eliminates the need for expensive sensors by relying on astronomical equations, resulting in a more affordable and accessible solution.

(2). The solar tracker showcases real-time adjustments, precisely following the sun's path and dynamically adapting to changing solar angles throughout the day.

(3). By incorporating shadow length measurements, the solar tracker effectively avoids shading, ensuring continuous exposure to sunlight and maximizing energy absorption.

(4). The design simplicity makes the solar tracker easy to implement, reducing installation complexities and associated costs.

(5). With minimal electronic and mechanical components, the sensorless solar tracker requires less maintenance, contributing to long-term reliability.

(6). The ability to accurately track the sun without reliance on sensors optimizes solar panel orientation, leading to increased energy productivity.

(7). The design's effectiveness in enhancing PV building integrated systems makes it a practical and efficient solution for integrating solar energy into various architectural structures.

(8). The designed solar tracker is efficient, as it consumes only 2.7% of the energy produced, which is less than that of existing solar tracking systems.

As a future work, we aim to enhance the effectiveness of our shadow-avoidant solar tracker by implementing computer vision and machine learning techniques to continuously monitor the PV array's surroundings for new or moving obstacles such as growing trees or new structures. Additionally, we will add user-friendly software interfaces for remote monitoring and control to simplify management. Testing will be conducted on larger PV arrays in various regions with different climate conditions to ensure scalability and reliability. By tackling these challenges, we aim to further enhance the efficiency and reliability of solar energy systems, contributing to sustainable energy solutions across diverse applications.

REFERENCES

[1] SCISPACE. How much energy is consumed by buildings? https://typeset.io/questions/how-much-energy-is-consumed-by-buildings-6fi5l65bnt, accessed on March 15, 2024.

[2] Amarnath, N. Buildings can reduce energy intensity by up to 38%: Report. Facilities Dive. https://www.facilitiesdive.com/news/buildings-ener-gy-intensity-renewable-sustainability-report/704082/,

accessed on March 15, 2024.

[3] Masters, G.M. (2004). Photovoltaic materials and electrical characteristics. In Renewable and Efficient Electric Power Systems, John Wiley & Sons, pp. 445-504. https://doi.org/10.1002/0471668826.ch8

[4] Gonzalo, A.P., Marugán, A.P., Márquez, F.P.G. (2020). Survey of maintenance management for photovoltaic power systems. Renewable and Sustainable Energy Reviews, 134: 110347. https://doi.org/10.1016/j.rser.2020.110347

[5] Lappalainen, K., Valkealahti, S. (2020). Number of maximum power points in photovoltaic arrays during partial shading events by clouds. Renewable Energy, 152: 812-822. https://doi.org/10.1016/j.renene.2020.01.119

[6] Pillai, D.S., Rajasekar, N., Ram, J.P., Chinnaiyan, V.K. (2018). Design and testing of two phase array reconfiguration procedure for maximizing power in solar PV systems under partial shade conditions (PSC). Energy Conversion and Management, 178: 92-110. https://doi.org/10.1016/j.enconman.2018.10.020

[7] Hashemzadeh, S.M. (2019). A new model-based technique for fast and accurate tracking of global maximum power point in photovoltaic arrays under partial shading conditions. Renewable Energy, 139: 1061-1076. https://doi.org/10.1016/j.renene.2019.03.019

[8] Craciunescu, D., Fara, L. (2023). Investigation of the Partial shading effect of photovoltaic panels and optimization of their performance based on high-efficiency FLC algorithm. Energies, 16(3): 1169. https://doi.org/10.3390/en16031169

[9] Mamun, M.A.A., Hasanuzzaman, M., Selvaraj, J. (2017). Experimental investigation of the effect of partial shading on photovoltaic performance. IET Renewable Power Generation, 11(7): 912-921. https://doi.org/10.1049/iet-rpg.2016.0902

[10] Bayrak, F., Ertürk, G., Oztop, H.F. (2017). Effects of partial shading on energy and exergy efficiencies for photovoltaic panels. Journal of Cleaner Production, 164: 58-69. https://doi.org/10.1016/j.jclepro.2017.06.108

[11] Swaleh, M.S., Green, M.A. (1982). Effect of shunt resistance and bypass diodes on the shadow tolerance of solar cell modules. Solar Cells, 5(2): 183-198. https://doi.org/10.1016/0379-6787(82)90026-6

[12] Vieira, R.G., de Araújo, F.M., Dhimish, M., Guerra, M.I. (2020). A comprehensive review on bypass diode application on photovoltaic modules. Energies, 13(10): 2472. https://doi.org/10.3390/en13102472

[13] Pannebakker, B.B., de Waal, A.C., van Sark, W.G. (2017). Photovoltaics in the shade: One bypass diode per solar cell revisited. Progress in Photovoltaics: Research and Applications, 25(10): 836-849. https://doi.org/10.1002/pip.2898

[14] Silvestre, S., Boronat, A., Chouder, A. (2009). Study of bypass diodes configuration on PV modules. Applied Energy, 86(9): 1632-1640. https://doi.org/10.1016/j.apenergy.2009.01.020

[15] Fadliondi, F., Isyanto, H., Budiyanto, B. (2018). Bypass diodes for improving solar panel performance. International Journal of Electrical and Computer Engineering, 8(5): 2703-2708.

[16] Vemuru, S., Singh, P., Niamat, M. (2012). Modeling impact of bypass diodes on photovoltaic cell performance under partial shading. In 2012 IEEE International Conference on Electro/Information Technology, Indianapolis, IN, USA. https://doi.org/10.1109/EIT.2012.6220747

[17] Javed, K., Ashfaq, H., Singh, R. (2020). A new simple MPPT algorithm to track MPP under partial shading for solar photovoltaic systems. International Journal of Green Energy, 17(1): 48-61. https://doi.org/10.1080/15435075.2019.1686001

[18] Mohapatra, A., Nayak, B., Das, P., Mohanty, K.B. (2017). A review on MPPT techniques of PV system under partial shading condition. Renewable and Sustainable Energy Reviews, 80: 854-867. https://doi.org/10.1016/j.rser.2017.05.083

[19] Kermadi, M., Salam, Z., Eltamaly, A.M., Ahmed, J., Mekhilef, S., Larbes, C., Berkouk, E.M. (2020). Recent developments of MPPT techniques for PV systems under partial shading conditions: A critical review and performance evaluation. IET Renewable Power Generation, 14(17): 3401-3417. https://doi.org/10.1049/iet-rpg.2020.0454

[20] Rizzo, S.A., Scelba, G. (2015). ANN based MPPT method for rapidly variable shading conditions. Applied Energy, 145: 124-132. https://doi.org/10.1016/j.apenergy.2015.01.077

[21] Ahmed, J., Salam, Z. (2014). A maximum power point tracking (MPPT) for PV system using cuckoo search with partial shading capability. Applied Energy, 119: 118-130. https://doi.org/10.1016/j.apenergy.2013.12.062

[22] Chen, K., Tian, S., Cheng, Y., Bai, L. (2014). An improved MPPT controller for photovoltaic system under partial shading condition. IEEE Transactions on Sustainable Energy, 5(3): 978-985. https://doi.org/10.1109/TSTE.2014.2315653

[23] Ramalu, T., Mohd Radzi, M.A., Mohd Zainuri, M.A.A., Abdul Wahab, N.I., Abdul Rahman, R.Z. (2016). A photovoltaic-based SEPIC converter with dual-fuzzy maximum power point tracking for optimal buck and boost operations. Energies, 9(8): 604. https://doi.org/10.3390/en9080604

[24] De Brito, M.A.G., Galotto, L., Sampaio, L.P., e Melo, G.D.A., Canesin, C.A. (2012). Evaluation of the main MPPT techniques for photovoltaic applications. IEEE Transactions on Industrial Electronics, 60(3): 1156-1167. https://doi.org/10.1109/TIE.2012.2198036

[25] Ramli, M.Z., Salam, Z. (2019). Performance evaluation of dc power optimizer (DCPO) for photovoltaic (PV) system during partial shading. Renewable Energy, 139: 1336-1354. https://doi.org/10.1016/j.renene.2019.02.072

[26] Lee, H., Choi, M., Kim, J., Kim, D., Bae, S., Yoon, J. (2023). Partial shading losses mitigation of a rooftop PV system with DC power optimizers based on operation and simulation-based evaluation. Solar Energy, 265: 112053. https://doi.org/10.1016/j.solener.2023.112053

[27] Wang, Q., Fang, J., Yao, W., Li, D., Ai, X., Wen, J. (2022). DC optimizer-based decentralized frequency support scheme of large-scale PV plants considering partial shading conditions. International Journal of Electrical Power & Energy Systems, 142: 108309. https://doi.org/10.1016/j.ijepes.2022.108309

[28] Lin, G., Bimenyimana, S., Tseng, M.L., Wang, C.H., Liu, Y., Li, L. (2020). Photovoltaic modules selection from shading effects on different materials. Symmetry, 12(12):

2082. https://doi.org/10.3390/sym12122082

[29] Akrami, M., Pourhossein, K. (2018). A novel reconfiguration procedure to extract maximum power from partially-shaded photovoltaic arrays. Solar Energy, 173: 110-119. https://doi.org/10.1016/j.solener.2018.06.067

[30] Dhanalakshmi, B., Rajasekar, N. (2018). A novel competence square based PV array reconfiguration technique for solar PV maximum power extraction. Energy Conversion and Management, 174: 897-912. https://doi.org/10.1016/j.enconman.2018.08.077

[31] Picault, D., Raison, B., Bacha, S., De La Casa, J., Aguilera, J. (2010). Forecasting photovoltaic array power production subject to mismatch losses. Solar Energy, 84(7): 1301-1309. https://doi.org/10.1016/j.solener.2010.04.009

[32] Tabanjat, A., Becherif, M., Hissel, D. (2015). Reconfiguration solution for shaded PV panels using switching control. Renewable Energy, 82: 4-13. https://doi.org/10.1016/j.renene.2014.09.041

[33] Subramanian, A., Raman, J. (2021). Grasshopper optimization algorithm tuned maximum power point tracking for solar photovoltaic systems. Journal of Ambient Intelligence and Humanized Computing, 12: 8637-8645. https://doi.org/10.1007/s12652-020-02593-9

[34] Rezazadeh, S., Moradzadeh, A., Pourhossein, K., Mohammadi-Ivatloo, B., Garcia Marquez, F.P. (2023). Photovoltaic array reconfiguration under partial shading conditions for maximum power extraction via knight's tour technique. Journal of Ambient Intelligence and Humanized Computing, 14(9): 11545-11567. https://doi.org/10.1007/s12652-022-03723-1

[35] Dhimish, M., Holmes, V., Mehrdadi, B., Dales, M., Chong, B., Zhang, L. (2017). Seven indicators variations for multiple PV array configurations under partial shading and faulty PV conditions. Renewable Energy, 113: 438-460. https://doi.org/10.1016/j.renene.2017.06.014

[36] Krishna, G.S., Moger, T. (2019). Reconfiguration strategies for reducing partial shading effects in photovoltaic arrays: State of the art. Solar Energy, 182: 429-452. https://doi.org/10.1016/j.solener.2019.02.057

[37] Yang, B., Yu, T., Zhang, X., Li, H., Shu, H., Sang, Y., Jiang, L. (2019). Dynamic leader based collective intelligence for maximum power point tracking of PV systems affected by partial shading condition. Energy Conversion and Management, 179: 286-303. https://doi.org/10.1016/j.enconman.2018.10.074

[38] Yousri, D., Allam, D., Eteiba, M.B. (2020). Optimal photovoltaic array reconfiguration for alleviating the partial shading influence based on a modified harris hawks optimizer. Energy Conversion and Management, 206: 112470. https://doi.org/10.1016/j.enconman.2020.112470

[39] Satpathy, P.R., Sharma, R. (2019). Power and mismatch losses mitigation by a fixed electrical reconfiguration technique for partially shaded photovoltaic arrays. Energy Conversion and Management, 192: 52-70. https://doi.org/10.1016/j.enconman.2019.04.039

[40] Sanseverino, E.R., Ngoc, T.N., Cardinale, M., Vigni, V.L., Musso, D., Romano, P., Viola, F. (2015). Dynamic programming and Munkres algorithm for optimal photovoltaic arrays reconfiguration. Solar Energy, 122: 347-358. https://doi.org/10.1016/j.solener.2015.09.016

[41] Yang, Z., Liao, K., Chen, J., Xia, L., Luo, X. (2021). Output performance analysis and power optimization of different configurations half-cell modules under partial shading. Optik, 232: 166499. https://doi.org/10.1016/j.ijleo.2021.166499

[42] Attia, O., Souissi, H., Khalil, M., Salah, C.B. (2021). Functioning of the half-cells photovoltaic module in hybrid EV under Partial Shading. In 2021 18th International Multi-Conference on Systems, Signals & Devices (SSD), Monastir, Tunisia, pp. 1252-1257. https://doi.org/10.1109/SSD52085.2021.9429410

[43] Pragallapati, N., Agarwal, V. (2013). Flyback configuration based micro-inverter with distributed MPPT of partially shaded PV module and energy recovery scheme. In 2013 IEEE 39th Photovoltaic Specialists Conference (PVSC), Tampa, FL, USA, pp. 2927-2931. https://doi.org/10.1109/PVSC.2013.6745079

[44] Mehedi, I.M., Salam, Z., Ramli, M.Z., Chin, V.J., Bassi, H., Rawa, M.J.H., Abdullah, M.P. (2021). Critical evaluation and review of partial shading mitigation methods for grid-connected PV system using hardware solutions: The module-level and array-level approaches. Renewable and Sustainable Energy Reviews, 146: 111138. https://doi.org/10.1016/j.rser.2021.111138

[45] Ahmed, J., Salam, Z. (2017). An accurate method for MPPT to detect the partial shading occurrence in a PV system. IEEE Transactions on Industrial Informatics, 13(5): 2151-2161. https://doi.org/10.1109/TII.2017.2703079

[46] Cardinale-Villalobos, L., Meza, C., Murillo-Soto, L.D. (2020). Experimental comparison of visual inspection and infrared thermography for the detection of soling and partial shading in photovoltaic arrays. In Ibero-American Congress of Smart Cities. Cham: Springer International Publishing, pp. 302-321. https://doi.org/10.1007/978-3-030-69136-3_21

[47] Henry, C., Poudel, S., Lee, S.W., Jeong, H. (2020). Automatic detection system of deteriorated PV modules using drone with thermal camera. Applied Sciences, 10(11): 3802. https://doi.org/10.3390/app10113802

[48] Mazumdar, D., Biswas, P.K., Sain, C., Ahmad, F., Ustun, T.S., Kalam, A. (2024). Performance analysis of drone sqadron optimisation based MPPT controller for grid implemented PV battery system under partially shaded conditions. Renewable Energy Focus, 49: 100577. https://doi.org/10.1016/j.ref.2024.100577

[49] Bocullo, V., Martišauskas, L., Pupeikis, D., Gatautis, R., Venčaitis, R., Bakas, R. (2023). UAV photogrammetry application for determining the influence of shading on solar photovoltaic array energy efficiency. Energies, 16(3): 1292. https://doi.org/10.3390/en16031292

[50] Rouani, L., Harkat, M.F., Kouadri, A., Mekhilef, S. (2021). Shading fault detection in a grid-connected PV system using vertices principal component analysis. Renewable Energy, 164: 1527-1539. https://doi.org/10.1016/j.renene.2020.10.059

[51] Kuhn, P., Wilbert, S., Prahl, C., Schüler, D., Haase, T., Hirsch, T., Wittmann, M., Ramirez, L., Zarzalejo, L., Meyer, A., Vuilleumier, L., Blanc, P., Pitz-Paal, R. (2017). Shadow camera system for the generation of solar irradiance maps. Solar Energy, 157: 157-170. https://doi.org/10.1016/j.solener.2017.05.074

[52] Bidram, A., Davoudi, A., Balog, R.S. (2012). Control

and circuit techniques to mitigate partial shading effects in photovoltaic arrays. IEEE Journal of Photovoltaics, 2(4): 532-546. https://doi.org/10.1109/JPHOTOV.2012.2202879

[53] Yang, B., Ye, H., Wang, J., Li, J., Wu, S., Li, Y., Shu, H., Ren, Y., Ye, H. (2021). PV arrays reconfiguration for partial shading mitigation: Recent advances, challenges and perspectives. Energy Conversion and Management, 247: 114738. https://doi.org/10.1016/j.enconman.2021.114738

[54] Kreft, W., Filipowicz, M., Żołądek, M. (2020). Reduction of electrical power loss in a photovoltaic chain in conditions of partial shading. Optik, 202: 163559. https://doi.org/10.1016/j.ijleo.2019.163559

[55] Gielen, D., Boshell, F., Saygin, D., Bazilian, M.D., Wagner, N., Gorini, R. (2019). The role of renewable energy in the global energy transformation. Energy Strategy Reviews, 24: 38-50. https://doi.org/10.1016/j.esr.2019.01.006

[56] Osman, I.S., Almadani, I.K., Hariri, N.G., Maatallah, T.S. (2022). Experimental investigation and comparison of the net energy yield using control-based solar tracking systems. International Journal of Photoenergy, 2022(1): 7715214. https://doi.org/10.1155/2022/7715214

[57] Kuttybay, N., Saymbetov, A., Mekhilef, S., Nurgaliyev, M., Tukymbekov, D., Dosymbetova, G., Meiirkhanov, A., Svanbayev, Y. (2020). Optimized single-axis schedule solar tracker in different weather conditions. Energies, 13(19): 5226. https://doi.org/10.3390/en13195226

[58] Ahmad, S., Shafie, S., Ab Kadir, M.Z.A. (2013). Power feasibility of a low power consumption solar tracker. Procedia Environmental Sciences, 17: 494-502. https://doi.org/10.1016/j.proenv.2013.02.064

[59] Mousazadeh, H., Keyhani, A., Javadi, A., Mobli, H., Abrinia, K., Sharifi, A. (2009). A review of principle and sun-tracking methods for maximizing solar systems output. Renewable and Sustainable Energy Reviews, 13(8): 1800-1818. https://doi.org/10.1016/j.rser.2009.01.022

[60] Khatib, T., Elmenreich, W. (2016). Modeling of Photovoltaic Systems Using Matlab: Simplified Green Codes. John Wiley & Sons. Hoboken, New Jersey: Wiley-Blackwell. https://doi.org/10.1002/9781119118138

[61] NASA POWER. Data Access Viewer. https://power.larc.nasa.gov/data-access-viewer/, accessed on June 29, 2023.

NOMENCLATURE

a	Shadow length
AST	Apparent solar time
B	Angle of declination
b	Building height
d	Number of days elapsed
EoT	Difference between apparent and mean solar times
h	Hour angle
LST	Local solar time
t	Time
TC	Time correction factor
Z_S	Azimuth angle
α	Altitude angle
β	Tilt angle
δ	Declination angle
λ	Longitude
ω	Angular displacement of the sun from the local point
$θ_z$	Zenith angle